

# Helium-Air Exchange Flow with Fluids Interaction

T. I. Kang\*

유체간섭을 동반하는 헬륨과 공기의 치환류  
강 태 일

**Key words** : HTGR (High Temperature Gas Cooled Reactor), Exchange Flow, Fluids Interaction, Two-Opening, Mach-Zehnder Interferometer

## Abstract

This paper describes experimental investigations of helium-air exchange flows through partitioned opening and two-opening. Such exchange flows may occur following rupture accident of stand pipe in high temperature gas cooled reactor. A test vessel with the two types of small opening on top of test cylinder is used for experiments. An estimation method of mass increment is developed and applied to measure the exchange flow rate. A technique of flow visualization by Mach-Zehnder interferometer is provided to recognize the exchange flows. In the case of exchange flow through the partitioned opening, flow passages of upward flow of the helium and downward flow of the air within the opening are separated by vertical partition, and the two flows interact out of entrance and exit of the opening. Therefore, an experiment of the exchange flow through two-opening is made to investigate effect of the fluids interaction of the partitioned opening system. As a result of comparison of the exchange flow rates between the two types of the opening system, it is found that the exchange flow rate of the two-opening system is larger than that of the partitioned opening system due to absence of the effect of fluids interaction. Finally, the fluids interaction between the upward and downward flows through the partitioned opening is found to be an important factor on the helium-air exchange flow.

## 1. Introduction

In safety study of a high temperature gas cooled reactor (HTGR), rupture of stand pipes

at top of the reactor vessel is considered as one of the most critical design-base accidents<sup>1)</sup>. Figure 1 shows a schematic drawing of the HTGR and the HTGR is a graphite moderated high

\* Chang Shin College (Receipt : Oct. '96)

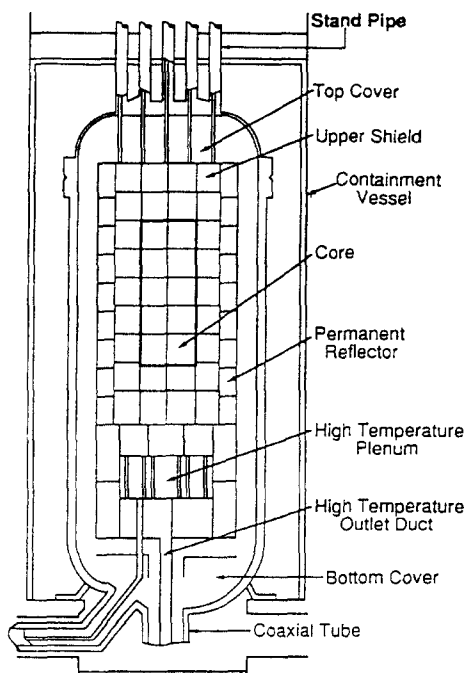


**Fig. 1 Schematic diagram of HTGR's arrangement**

temperature gas-cooled reactor of 30 MW thermal power and 950 °C outlet helium coolant temperature. When stand pipes rupture, helium coolant gas in high pressure flows immediately through breach out of the reactor vessel. After the pressure in the reactor vessel has fallen to that of the atmosphere, the air flows into the reactor vessel, which is caused by buoyancy force due to density difference between the helium inside the reactor vessel and the air outside. The penetrated air reacts with high temperature graphite structure, and causes corrosion of the graphite components, which results in a severe damage of in-core reactor structures. Therefore, an estimation of magnitude of the buoyancy-driven exchange flow through the stand pipe is necessary to assess the air flow into the reactor vessel.

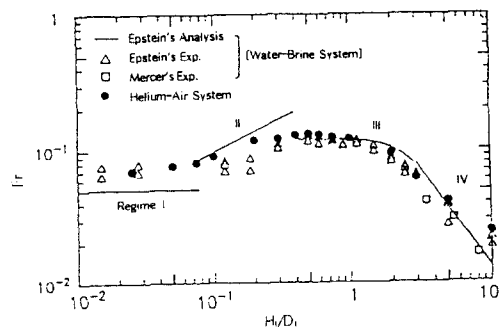


**Fig. 2 Comparison of measured Froude numbers between helium-air system and brine-water system<sup>8)</sup>**

From a survey of the literature, it appeared that some papers dealt with buoyancy-driven exchange flow with brine-water<sup>2-5)</sup> and air-air<sup>6-7)</sup>. Epstein<sup>2)</sup> made measurements of the buoyancy-driven exchange flow with a single opening, for opening ratios  $H_1/D_1$  in the range 0.01 to 10, where  $H_1$  and  $D_1$  are height of the opening and inner diameter of the opening, respectively. He suggested four different flow regimes shown in Fig. 2, as  $H_1/D_1$  increased through this range. As a result of these measurements, he found a peak value of the exchange flow rate at  $H_1/D_1$  of about 0.5 as shown in Fig. 2. Most of the above studies on the buoyancy-driven exchange flow have been carried out with a single opening and small density difference. However, the density of cold air outside reactor vessel is at least three times larger than that of gas mixture (helium and hot air) inside the reactor vessel at the stand pipe rupture accident. Fumizawa<sup>8)</sup> conducted experiments for the Epstein's experimental conditions with the helium-air and the single opening. He reported that the experimental results for the helium-air system agreed with those for the Epstein's brine-water system as shown in Fig. 2. In Epstein's paper<sup>2)</sup>, he also made experiments with two openings. His experimental purpose was to investigate flow patterns of the two-opening

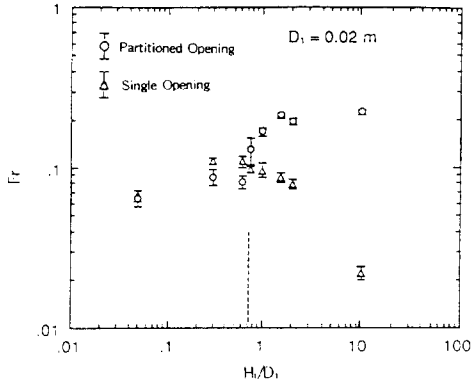


Fig. 3 Comparison of measured Froude numbers between single opening system and partitioned opening system<sup>9)</sup>

system, and the two openings were observed to give rise to three different flow configurations. There were no studies for the exchange flow through partitioned opening (opening with a vertical partition) in the previous studies of the buoyancy-driven exchange flow. Kang et al.<sup>9)</sup> performed experiments on the helium-air exchange flow with the partitioned opening and the single opening for opening ratios  $H_1/D_1$  in the range 0.05 to 10 as shown in Fig. 3. From a fundamental point of view, there is a big difference of flow passages between the partitioned opening and the single opening. Thus, it is necessary to compare exchange flow rate and flow pattern between the two types of opening. At lower opening ratios ( $H_1/D_1 < 0.75$ ), the exchange flow rates for the partitioned opening system were almost the same as those for the single opening system. However, at higher opening ratios ( $H_1/D_1 \geq 0.75$ ), they were larger than those for the single opening system, because upward flow of the helium and downward flow of the air were separated by the vertical partition within the opening. Effect of the various inner diameters of the opening on the exchange flow rate was investigated at higher opening ratios in Fig. 4<sup>10)</sup>. The inner diameters

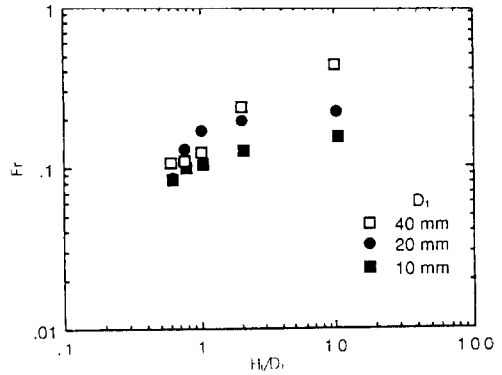


Fig. 4 Effect of opening diameter on measured Froude number<sup>10)</sup>

of the opening were 0.01, 0.02, and 0.04 m, and the opening ratios were in the range 0.6 to 10. The exchange flow rates increased with increasing the inner diameter. Based on his flow visualizations<sup>9-10)</sup>, he pointed out the effect of fluids interaction between the air and the helium out of entrance and exit of the partitioned opening. Therefore, in this study, an experiment with two-opening system is performed to confirm the fluids interaction of the partitioned opening system on the exchange flow. And also, to explain trend of the exchange flow rate of the two-opening system, loop flow in test vessel is discussed.

## 2. Experimental Apparatus and Procedures

Figure 5 illustrates an experimental apparatus to evaluate the exchange flow rate for the partitioned opening system and two-opening system. Essential features of the experimental apparatus are described with aid of Fig. 5. The experimental apparatus is composed of a test vessel, an electronic balance, and a personal computer for data acquisition. The test vessel consists of a test cylinder and opening made

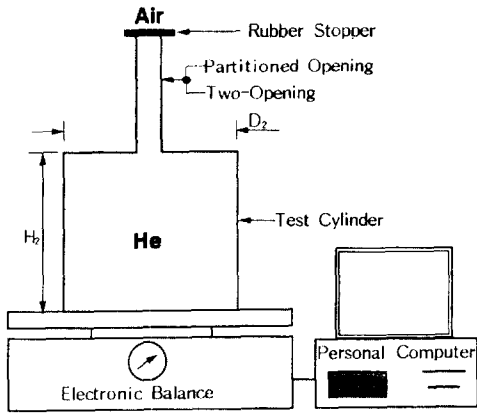


Fig. 5 Schematic diagram of experimental apparatus

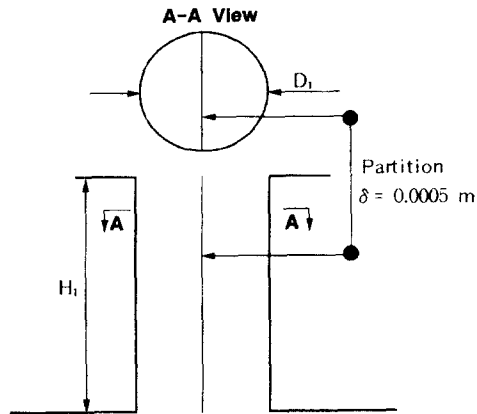


Fig. 6 Schematic diagram of partitioned opening

from plexiglass. Two types of the opening were employed in the experiments, i.e., the partitioned opening and the two-opening. The opening configurations studied are presented in Fig. 6 and Fig. 7. A vertical partition of rectangular plate is in alignment with center line of the opening to make the partitioned opening as shown in Fig. 6, where partition thickness is 0.0005 m. Figure 7 shows a test section for confirming the effect of fluids interaction of the partitioned opening system on the exchange flow rate. Each opening is separated by the vertical partition. A distance (0.1 m) between the

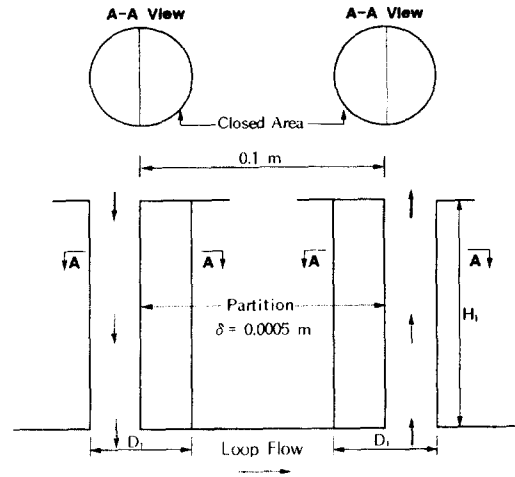


Fig. 7 Schematic diagram of two-opening and loop flow model

two openings is long enough to remove the fluids interaction between the upward flow of the helium and downward flow of the air. One side of each opening is closed to avoid the fluids interaction. The diameters and heights of the openings and the test cylinders are described in Table 1. The experiments were carried out

Table 1. Test Vessel Geometry

Opening Type	$D_1$ m	$H_1$ m	$D_2$ m	$H_2$ m
Partitioned Opening	0.01	0.1	0.1	0.2
Two - Opening	0.01	0.1	0.194	0.4

under the atmospheric pressure and room temperature. The test vessel was filled with pure helium gas initially. The opening's top was sealed with a thin rubber stopper as shown in Fig. 5. On removal of rubber stopper placed on the top of the opening, the buoyancy-driven exchange flow was initiated and the heavier air was introduced into the test vessel. Thus, the mass of gas mixture in the test vessel increased. Figure 8 shows optical components of Mach-Zehnder interferometer to visualize the exchange flow. Illumination beam (He-Ne

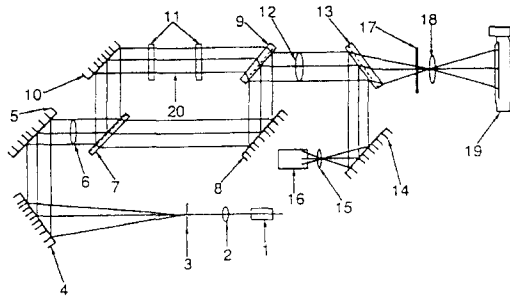


**Fig. 8 Optical components of Mach-Zehnder interferometer**

- |                |              |                 |                  |
|----------------|--------------|-----------------|------------------|
| 1. Laser       | 2. Lens 1    | 3. Pinhole      | 4. Mirror 1      |
| 5. Mirror 2    | 6. Lens 2    | 7. Splitter 1   | 8. Mirror 3      |
| 9. Splitter 2  | 10. Mirror 4 | 11. Window      | 12. Lens 3       |
| 13. Splitter 3 | 14. Mirror 5 | 15. Lens 4      | 16. CCD Camera   |
| 17. Screen     | 18. Lens 5   | 19. 35mm Camera | 20. Test Section |

laser supplied from light source, wave length 633 nm) collimated by lens 2 is split by beam splitter 1 inclined at 45° into a test beam and a reference beam. The test beam reflected by coated surface of the beam splitter 1 is reflected by mirror 4 in order to cross the test section closed by windows. The beam is then transmitted through the beam splitter 2, forming a test section image on observation screen. At the same time, the reference beam transmitted through the beam splitter 1 is successively reflected by mirror 3 and coated surface splitter 2 before being superimposed on the test beam, the beam splitter 2 imposes the same optical path delay on the test beam that the beam splitter 1 does on the reference one. Consequently, the test beam and the reference beam are mixed beyond the beam splitter 2. The test beam and the reference beam interfere, and interference fringe pattern appears on the screen. If density of the test section is homogeneous, straight parallel equidistant interference fringes appear<sup>(1)</sup>. If it is inhomogeneous, distorted interference fringes appear. The experimental procedure of two-opening system was essentially the same as that

described in the foregoing for the partitioned opening system, except that the two rubber stoppers were placed, one in each opening. Three programs, i.e., program for measuring mass increment, program for calculation of density increment, and program for calculation of measured Froude number are used for data processing in the present experiment. The flow was initiated by removing each stopper simultaneously. The mass increment  $\Delta m_t$  of the gas mixture was measured by means of the electronic balance at regular intervals.

$$\Delta m_t = m_{M_t} - m_{H_2O} \quad (1)$$

The gas mixture's density increment  $\Delta \rho_L$  is calculated from the mass increment, and it is given by

$$\Delta \rho_L = \frac{\Delta m_t}{V} \quad (2)$$

, where  $V^{st}$  is volume of the test vessel. The volume exchange flow rate  $Q$  through the opening is evaluated by the measured density increment. Mass balance on the gas mixture gives

$$V \frac{d\Delta \rho_L}{dt} = Q \rho_H - Q \rho_L \quad (3)$$

The volume exchange flow rate is expressed in the form of a Froude number  $Fr$ , and it is defined as

$$Fr = Q \sqrt{\frac{\rho_m}{D_f^5 g (\rho_H - \rho_L)}} \quad (4)$$

In the present experiment, the effective diameter  $D_f$  is used in Eq. (4) because the openings are not round, and it is given by

$$D_f = \sqrt{\frac{4}{\pi} \left( \frac{\pi D_1^2}{4} - D_1 \delta \right)} \quad (5)$$

### 3. Results and Discussion

Figure 9 illustrates variation of the density increment with time, and the inner diameter of the opening is 0.01 m. The density increment for both opening systems increases with time. As expressed in Eq. (2), the density increment of the gas mixture in the test vessel increases due to the exchange flow. Finally, it approaches the density difference between the air and the helium. The density increment of the partitioned opening system is larger than that of the two-opening system because the volume of the test vessel with partitioned opening is smaller

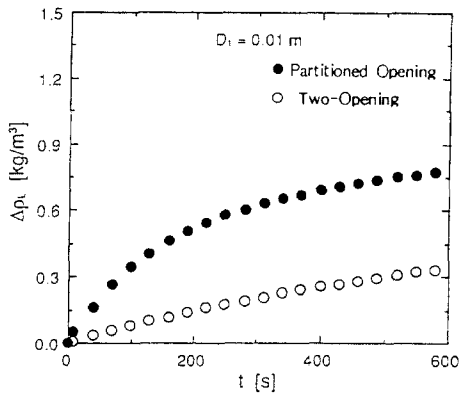


Fig. 9 Variation of density increment with time

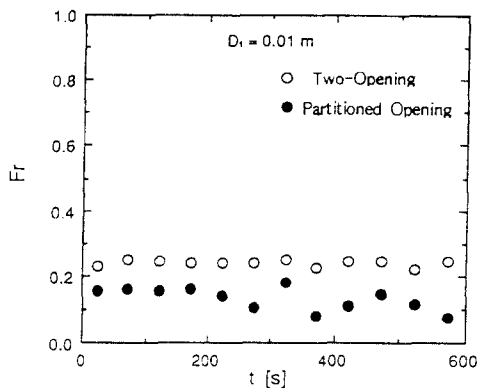


Fig.10 Variation of Froude number with time

than that of the test vessel with the two-opening as shown in Table 1. Figure 10 shows variation of the measured Froude number with time. The measured Froude number of the two-opening system is almost constant with time because it is thought that buoyancy force, i.e., the density difference between the air and the gas mixture is almost constant. The measured Froude number of the partitioned opening system appears to be constant value before about 200 second. They fluctuate after about 200 second and thus, these measured data are not sufficient to explain the trend of the exchange flow rate. Discussion of figure 10 is described in Fig. 11 again. Figure 10 shows that difference in the measured Froude numbers between the two-opening system and the partitioned opening system results from the effect of fluids interaction. Figure 11 is prepared to illustrate the comparison of relationship between the measured Froude number and the density increment. This figure shows the variations of measured Froude number for both opening systems are less than 9% in the range of  $0 \leq \Delta\rho_L \leq 0.5 \text{ kg/m}^3$ . Therefore, in the present experiment, the Froude number in Table 2 is defined as the average value of the measured Froude

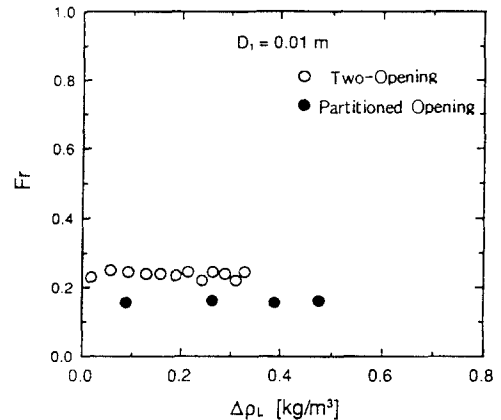
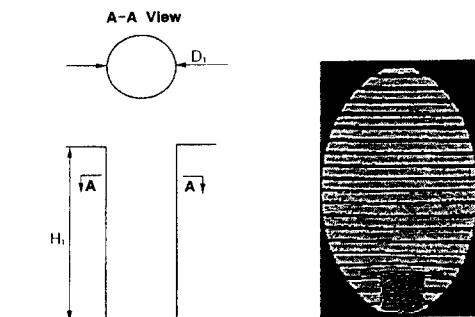


Fig.11 Variation of Froude number with density increment

**Table 2. Comparison of Froude numbers between two types of opening system**

Opening Type	Froude number
Two - Opening	0.2381
Partitioned Opening	0.1571

numbers in the range of  $0 \leq \Delta\rho_L \leq 0.5 \text{ kg/m}^3$ . As was already mentioned, experiments for flow visualization were conducted by Mach-Zehnder interferometer to compare flow patterns. For our understanding of the flow visualization of the helium-air exchange flow, an example of interference fringe pattern of the single opening system (no partition,  $H_1/D_1=10$ ) is introduced in Fig. 12. In the case of  $Fr \rightarrow 0$ , the distorted interference fringes do not appear because there is almost no exchange flow as shown in Fig. 12. Figure 13 shows Mach-Zehnder interferograms of fringes of the air and the gas mixture for the partitioned opening system and the two-opening system at  $H_1/D_1$  of 10. The distorted interference fringes show that the gas mixture flows out of the opening and the straight fringes indicate that the air flows into the opening. According to observations by video camera, the gas mixture flows out of any open-



**Fig.12 Example of flow visualization of single opening system with Mach-Zehnder interferometer**

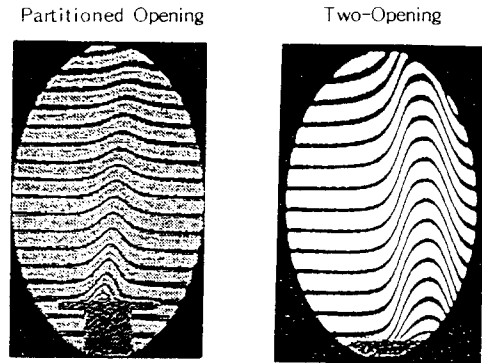


**Fig.13 Comparison of flow visualizations with Mach-Zehnder interferometer**

ing of the two-opening system and the fringes of the gas mixture do not fluctuate laterally as shown in Fig. 13. It means that the flow of the gas mixture is stably separated from the air flow out of the opening due to absence of the fluids interaction and this leads to less resistance for the exchange flow of the two-opening system, as compared with the exchange flow of the partitioned opening system. Therefore, the exchange flow rate of two-opening system is larger than that of the partitioned opening system as shown in Table 2. However, the gas mixture flow of the partitioned opening system swings a little from left to right in lateral direction out of the entrance of the opening, and condition of the exchange flow at the opening entrance is observed to be unstable as shown in Fig. 13. It indicates that the fluids interaction takes place as a main resistance to the exchange flow. To explain another reason that the exchange flow rate of the two-opening system is larger than that of the partitioned opening system, an influence of loop flow to expedite the exchange flow is suggested. It is apparent from closely related work reported in the literature that the loop flow expedites the exchange flow<sup>2)</sup>. Experiments with brine-water on the loop flow through two openings were reported

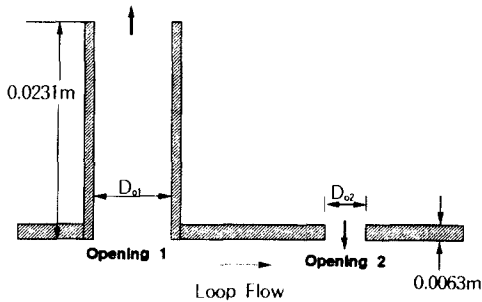


Fig.14 Schematic diagram of loop flow observed by Epstein in two-opening system <sup>2)</sup>

by Epstein<sup>2)</sup>. A total of nine experiments were performed with the two openings, and in this paper, eight cases are introduced for the discussion. In his experiments, height and  $D_{01}$  of opening 1 were fixed and ratio of flow area  $A_{01}/A_{02}$  was varied by making use of different opening 2 diameters  $D_{02}$  as shown in Table 3, where  $A_{01}$  is the flow area of the opening 1 and  $A_{02}$  is the flow area of the opening 2. The openings were separated by a distance approximately 0.15 m in his experiment. These experiments were designed to observe flow patterns in inside of the test vessel as  $D_{02}$  increased. He suggested two different flow configurations by  $A_{02}/A_{01}$  parameter in the range 0.09 to 25.63. One is bidirectional flow within opening 1 and unidirectional flow within opening 2, and the other is the loop flow to expedite the exchange flow was observed at  $A_{02}/A_{01} \geq 0.7485$  in his

Table 3. Experimental condition of loop flow occurrence <sup>2)</sup>

Expt. No.	$D_{01}$ m	$D_{02}$ m	Reference
1	0.0445	0.0127	
2	0.0445	0.0191	
3	0.0445	0.0294	
4	0.0445	0.0353	
5	0.0445	0.0385	Loop Flow
6	0.0445	0.0445	Loop Flow
7	0.0445	0.0516	Loop Flow
8	0.0445	0.0643	Loop Flow

experiment as shown in Fig. 14. Therefore, we suggest that the loop flow may occur as shown in schematic view of Fig. 7, because the ratio of flow area  $A_{02}/A_{01}$  is 1 in this experiment. And thus, we think that it is another mechanism to expedite the exchange flow. The flow visualization of the loop flow within the test vessel is not prepared at present stage and thus, it will be necessary to confirm the loop flow in the helium-air exchange flow at next stage as a further study.

#### 4. Conclusions

An experimental study of the helium-air exchange flows through the partitioned opening and two-opening has been carried out in order to understand characteristics of the penetrated air flow at the rupture accident of the stand pipe in the HTGR. In this paper, the effect of fluids interaction on the exchange flow was confirmed experimentally and discussed. Conclusions of this paper are summarized in three groups as follow :

1) The fluids interaction between upward and downward flows out of the entrance and the exit of the partitioned opening is found to be an important factor on the helium-air exchange flow.

2) The exchange flow rate of the two-opening system is larger than that of the partitioned opening system due to the absence of the fluids interaction.

3) The present study is useful in understanding helium-air exchange flow at the rupture accident of the stand pipe in the HTGR.

Further study will be required to explain the fluids interaction quantitatively and the flow patterns inside the two-opening system.



## Nomenclature

$A_{o1}$	flow area of opening 1 in reference [2] ( $m^2$ )
$A_{o2}$	flow area of opening 2 in reference [2] ( $m^2$ )
$D_1$	inner diameter of opening (m)
$D_r$	effective diameter of opening (m)
$D_{o1}$	inner diameter of opening 1 in reference [2] (m)
$D_{o2}$	inner diameter of opening 2 in reference [2] (m)
$Fr$	Froude number
$g$	acceleration due to gravity ( $m/s^2$ )
$H_1$	height of opening (m)
$m$	mass (kg)
$\Delta m$	mass increment (kg)
$Q$	volume exchange flow rate ( $m^3/s$ )
$t$	elapsed time (s)
$V$	volume of test vessel ( $m^3$ )
$\delta$	partition thickness (m)
$\rho$	density ( $kg/m^3$ )
$\rho_m$	mean density = $(\rho_H + \rho_L)/2$ ( $kg/m^3$ )
$\Delta\rho_L$	density increment ( $kg/m^3$ )

## Subscripts

H	heavier fluid (air)
He	helium
L	light fluid (gas mixture)
M	gas mixture
t	elapsed time
0	initial condition

## Acknowledgments

The author wishes to thank Dr. M. Fumizawa of Japan Energy Research Institute and Dr. Yun Won-Young of Korea Institute of Nuclear Safety for a number of useful discussions. The author also wishes to thank Ms. N. Kanzaki of the University of Tokyo for her administrative assistances.

## References

- 1) JAERI, "Present Status of HTGR Research and Development," JAERI Report, (1992).
- 2) M. Epstein, "Buoyancy-Driven Exchange Flow Through Small Openings in Horizontal Partitions," *Trans. of ASME*, Vol. 110, 885 (1998).
- 3) A. Mercer, and H. Thompson, "The Exchange Flow in Inclined Ducts," *J. Br. Nucl. Energy Soc.*, Vol. 14, 327 (1975).
- 4) A. Mercer, and H. Thompson, "The Purging Flow in Inclined Ducts," *J. Br. Nucl. Energy Soc.*, Vol. 14, 330 (1975).
- 5) S. J. Leach, and H. Thompson, "An Investigation of Some Aspects of Flow into Gas Cooled Nuclear Reactors Following an Accidental Depressurization," *J. Br. Nucl. Energy Soc.*, Vol. 14, 243 (1975).
- 6) W. G. Brown, and K. R. Solvason, "Natural Convection Through Rectangular Openings in Partitions-1," *Int. J. Heat Mass Transfer*, Vol. 5, 859 (1962).
- 7) W. G. Brown, and K. R. Solvason, "Natural Convection Through Rectangular Openings in Partitions-2," *Int. J. Heat Mass Transfer*, Vol. 5, 869 (1962).
- 8) M. Fumizawa et al., "Experimental Study of Helium-Air Exchange Flow Through a Small Opening," *Kerntechnik*, Vol. 57, 156 (1992).
- 9) T. I. Kang et al., "Helium-Air Exchange Flow Through a Partitioned Vertical Opening with a Partition," *Proc. 5th Int. Topical Meeting on Nuclear Reactor Thermal Hydraulics*, Salt Lake City, Vol. II, 541 (1993).
- 10) T. I. Kang et al., "Helium-Air Exchange Flow Through Multiple Openings," *Proc. 6th Int. Symposium on Transport Phenomena*, Seoul City, Vol. I, 325 (1993).
- 11) W. J. Yang, *Handbook of Flow Visualization*, 2nd ed., p. 205, Hemisphere Publishing Corporation, New York (1989).